Check for updates

Accepted Article

A Comprehensive Monte Carlo Model of the Grafting of Maleic Anhydride onto Polypropylene with Experimental Validation

Tomás Romero Pietrafesa, Adriana Brandolin, Claudia Sarmoria, and Mariano Asteasuain*

T. Romero Pietrafesa, C. Sarmoria, M. Asteasuain

PLAPIQUI (UNS-CONICET), Camino La Carrindanga km 7, Bahía Blanca (8000), Buenos Aires, Argentina

Departamento de Ingeniería Química, Universidad Nacional del Sur, Av. Alem 1253, Bahía Blanca (8000), Buenos Aires, Argentina

masteasuain@plapiqui.edu.ar

A. Brandolin

PLAPIQUI (UNS-CONICET), Camino La Carrindanga km 7, Bahía Blanca (8000), Buenos Aires, Argentina

Keywords: polypropylene, maleic anhydride, graft, copolymer, model, Monte Carlo, Response Surface method.

Abstract

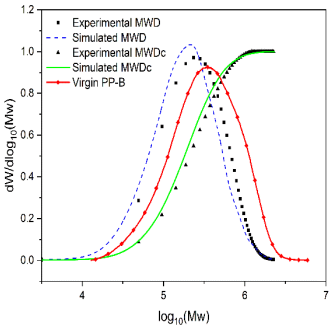
A Monte Carlo model was employed to investigate the grafting of maleic anhydride onto polypropylene using a peroxide initiator. The study aimed to develop a comprehensive model that considered a very detailed kinetic mechanism, including chain transfer to polymer, homopolymerization as well as several copolymer reactions. The relative importance of these reactions was evaluated using a sensitivity analysis, which identified homopolymerization, β-scission, chain grafting, and termination by disproportionation as the most influential reactions. The kinetic constants of these reactions were tuned to fit reported experimental data using the Surface Response Method. The model considers a pseudo-homogeneous reaction medium and predicts average molecular weights, degree of grafting, molecular weight distribution, and grafting distribution. Furthermore, model simulations provided useful information about the impact of initial concentrations of reactants and reaction time on the molecular properties of the grafted polymer.

We present a Monte Carlo model for the grafting of maleic anhydride onto polypropylene using peroxide as initiator. We perform a sensitivityy analysis to evaluate which kinetic steps affect polymer properties the most. The final set of contants allows fitting experimental data. The model is used to assess effects of initial concentrations and reaction time on polymer properties.

This article has been accepted for publication and undergone full peer review but has not been through the copyediting, typesetting, pagination and proofreading process, which may lead to differences between this version and the Version of Record. Please cite this article as doi: 10.1002/mats.202300018.

This article is protected by copyright. All rights reserved.

Accepted Article



1. Introduction

For several decades, research has been conducted on the grafting reactions of unsaturated monomers on polypropylene (PP). Functionalization of PP through the grafting of a comonomer helps to obtain desired properties while improving other features. The use of maleic anhydride (MAH) as a graft monomer is well documented[1-3] and has been shown to improve physical properties and enhance compatibility with polymer blends such as polyamides and polyesters. The PP-g-MAH also allows further modifications to create special polymer structures, such as branching.[4-6] Numerous experimental studies have been published on the entire grafting process,[7-23] using a variety of production methods, with reactive extrusion being the most commonly used technique.[7] These studies provide valuable information on the characterization of the reaction system and highlight the influence of the process variables on the final properties of the copolymer. It is worth mentioning that numerous studies regarding the grafting of various polymers to alter their properties have been documented in the literature. These works provide valuable insights into the impact and significance of grafting.[24-27]

Despite the large number of works published on this subject, a complete understanding remains elusive and has been debated for many years. There is a consensus on the main steps of the grafting mechanism.[8-12, 28-32] The first step is the formation of radicals from peroxide decomposition. At relatively high temperatures, *β*-scission dominates, which is favored by the presence of radicals. In this reaction, two shorter chains are formed from one PP chain, one of which contains an end-chain radical, while the other chain becomes unsaturated. It is generally accepted that the grafting reaction can occur on any available radical and that there is termination by disproportionation reactions between PP molecules. However, several possible reactions in this process are not agreed upon. One of them is the homopolymerization of MAH. Some authors have disregarded its occurrence, citing the reaction's ceiling temperature,[10, 20] while others have reported the presence of a significant amount of MAH oligomer and suggested that the true ceiling temperature is higher than the previously reported one, which was a calculated value.[33, 34] A third, intermediate approach has also been

This article is protected by copyright. All rights reserved.

15213919, ja, Downloaded from https://onlinelibrary.wiley.com/doi/10.1002/mats.202300018 by MARIANO ASTEASUAIN - CONICET Consejo Nacional de Investigaciones , Wiley Online Library on [02/06/2023]. See the Terms and Conditions (https://onlinelibrary.wiley.com/terms-and-conditions) on Wiley Online Library for rules of use; OA articles are governed by the applicable Creative Commons License

Accepted Article

reported in which homopolymerization of MAH is allowed up to a certain chain length.[18] The occurrence of the hydrogen abstraction reaction remains a topic of debate. Some reports suggest that it is a step of the *β*-scission reaction,[33, 34] while others propose that it may occur independently, forming backbone radicals due to the large number of tertiary hydrogen atoms in the PP chains.[10, 35] The distinction between these two possibilities is crucial for understanding the reaction mechanism because the presence of backbone radicals broadens the spectrum of possible reactions. Other reactions, such as chain transfer to polymer and various forms of termination, are significant.[30, 31, 36, 37] It was also found that the *β*-scission reaction can also occur after the grafting reaction, leading to a combination of a copolymer radical and a dead chain.[37] This expands the possibilities for new reactions because the grafted copolymer has a different reactivity than the virgin PP.[30, 31, 37] Since the mixture contains both polar (MAH) and non-polar (PP) components, it is possible to describe it using two phases, or a single pseudo homogeneous phase. Previous studies have conducted a comparative analysis to assess the advantages of including phase differentiation in order to enhance the depiction of the grafting process.[25, 31, 38, 39] We found that for our system the use of a pseudo-homogeneous model was enough to accurately portray the grafting process, as we will discuss in detail later. Diffusional limitations have not been specially considered in this model. Although there are studies that highlight the importance of diffusional effects in grafting processes,[39] the approach adopted in this work represents the behavior of the system well, as evidenced by the comparison with experimental data. The influence of variables such as reaction time and reactant concentrations on the final properties, including the degree of grafting (*DG*), number-average molecular weight ($\overline{M_n}$), and weight average molecular weight ($\overline{M_w}$), is still a matter of debate. Nevertheless, some findings in this area have become widely accepted.[1-3, 7-9, 12-16, 19, 21-23, 28, 29, 35-37, 40-43]

Mathematical models that can accurately predict the molecular structure of the grafted polymer have become a desirable option for revealing the reaction mechanism. To achieve this, a comprehensive description of the reaction steps is required. There are numerous studies in the literature on the modeling of the grafting of MAH onto PP. For example, Giudici et al.[30] and Aguiar et al.[31] have developed a comprehensive mechanism encompassing a wide range of secondary reactions in single- and two-phase systems, respectively. These models were constructed using the method of moments, which transforms a system of population balance differential equations of infinite size into a finite system of moment equations. In these works, the method of moments provides information on the evolution of $\overline{M_n}$, $\overline{M_w}$, and *DG* over time, but it does not provide insight into other critical variables such as the rate of occurrence of the different reaction steps and the topology of the grafted chains. However, it is important to note that recent studies have reported being able to use the method of moments to determine the topology of polymer chains.[44, 45] Nevertheless, this method presents a

This article is protected by copyright. All rights reserved.

15213919, ja, Downloaded from https://onlinelibrary.wiley.com/doi/10.1002/mats.202300018 by MARIANO ASTEASUAIN - CONICET Consejo Nacional de Investigaciones , Wiley Online Library on [02/06/2023]. See the Terms and Conditions (https://onlinelibrary.wiley.com/terms-and-conditions) on Wiley Online Library for rules of use; OA articles are governed by the applicable Creative Commons License

Accepted Article

challenge when dealing with reactions such as *β*-scission and chain transfer to polymer, as it requires closure equations for the resulting open system of moment equations. Shi et al.[29] and Zhu et al.[32] presented Monte Carlo (MC) algorithms based on a simplified reaction mechanism that did not consider many of the possible secondary reactions. Although these two studies are consistent with each other and show good agreement with experimental data, they fell short of giving a full comprehension of the reaction mechanism and determining the relative significance of the reactions that were presented.

A stochastic approach such as the MC method is well suited for this polymer system. It provides a thorough insight into the process variables as they change over time and can be easily refined by including additional kinetic steps, making it ideal for analyzing the effects of any secondary reaction. Several detailed analyses of the topography of grafts and polymer chain branches obtained using Monte Carlo methods have been reported.[24, 25, 44, 46, 47] In this work, a model is proposed that includes a comprehensive mechanism for grafting MAH onto PP. It is based on the MC approach and predicts the evolution along the reaction time of the number of molecules of each reacting species, the *DG*, the $\overline{M_n}$, $\overline{M_w}$, and molecular weight distribution (MWD) of the copolymer chains, as well as the chain length, position, and topology of the grafted MAH chains.

The model parameters were estimated using experimental data obtained in our laboratories. These data involved a variety of initial concentrations of MAH and peroxide, as well as measurements of $\overline{M_n}$, $\overline{M_w}$, MWD, and *DG* at different reaction times. First, a sensitivity analysis was performed to evaluate the effects of each kinetic step on the measured properties to identify the most important kinetic constants for the model validation. Then, the selected kinetic constants were tuned to fit the experimental data. A very good agreement was obtained. Afterward, the model was used to determine the influence of operating variables such as reaction time and reactant initial concentrations on the molecular properties of the polymer.

2. Kinetic mechanism

The system analyzed in this work is the grafting of MAH onto PP in bulk using 2,5-dimethyl-2,5-di-(tert-butyl peroxy) hexane as initiator. This initiator was selected due to its ability to generate four radicals per peroxide molecule, unlike other peroxides that produce fewer radicals per molecule. In addition, its half-liftime is suitable for the operating temperature and it is commonly used in PP modification.[8, 9, 12, 13, 17, 42, 43] The reaction was performed in a batch equipment, a Brabender Plastograph® mixer at 180 °C and 40 rpm. The experimental data were obtained in our laboratories. **Table 1** presents the initial concentrations of initiator and MAH, reaction time, and the average molecular weights and

This article is protected by copyright. All rights reserved.

15213919, ja, Downloaded from https://onlinelibrary.wiley.com/doi/10.1002/mats.202300018 by MARIANO ASTEASUAIN - CONICET Consejo Nacional de Investigaciones , Wiley Online Library on [02/06/2023]. See the Terms and Conditions (https://onlinelibrary.wiley.com/terms-and-conditions) on Wiley Online Library for rules of use; OA articles are governed by the applicable Creative Commons License

Accepted Article

degree of grafting of the grafted PP. Concentrations of reactants are defined as bulk concentrations considering the entire volume of the reaction medium. The initial concentration of the initiator is reported in parts per million (ppm), on a weight basis. Experiments E.I-E.III correspond to a virgin PP called PP-A of $\overline{M_n}$=1.06×10^5 g mol^{-1} and $\overline{M_w}$=3.82×10^5 g mol^{-1}; experiments E.IV and E.V correspond to a virgin PP called PP-B of $\overline{M_n}$=1.91×10^5 g mol^{-1} and $\overline{M_w}$=4.67×10^5 g mol^{-1}.

Table 1. Experimental data sets.

Experiment	Initiator [ppm]	MAH [w/w%]	Reaction time [min]	Copolymer $\overline{M_n}$ [g mol^{-1}]	Copolymer $\overline{M_w}$ [g mol^{-1}]	Degree of grafting [%]
E.I	375	1	5	98000	226000	0.058
E.II	750	1	10	81000	194000	0.106
E.III	750	1	40	46000	158000	0.125
E.IV	250	1	15	106000	314000	0.09
E.V	500	1	15	113000	290000	0.14

We present a thorough kinetic mechanism based on a literature review.[1-3, 7, 10-14, 17, 18, 20, 21, 23, 28-34, 36-38, 42, 48-50] To cover the largest possible number of reactions, we allow unrestricted homopolymerization of MAH in both grafted and ungrafted units. *β*-scission and chain transfer reactions are treated as described by De Roover et al.[33] In this approach, *β*-scission and chain transfer reactions are deemed to occur much faster than hydrogen abstraction reactions. As a result, these reactions (reactions (5)-(8) and (13)-(20)) are considered to happen simultaneously, leading to the generation of only end-chain radicals. Furthermore, these reactions create double bonds at the end of the inactive molecules, which are regarded as unreactive as reported in prior studies.[29-33, 38] Thermal degradation reactions were excluded because they only occur at temperatures much higher than the one used in our experiments.[51]

Peroxide decomposition

$$PO \xrightarrow{k_d} 4RO \quad (1)$$

Deactivation of initiation radicals

$$2RO \xrightarrow{k_{desro}} XRO \quad (2)$$

This article is protected by copyright. All rights reserved.

15213919, ja, Downloaded from https://onlinelibrary.wiley.com/doi/10.1002/mats.202300018 by MARIANO ASTEASUAIN - CONICET Consejo Nacional de Investigaciones , Wiley Online Library on [02/06/2023]. See the Terms and Conditions (https://onlinelibrary.wiley.com/terms-and-conditions) on Wiley Online Library for rules of use; OA articles are governed by the applicable Creative Commons License

Accepted Article

MAH activation

$$RO + MAH_{mon} \xrightarrow{k_{imah}} RMAH_1 \quad (3)$$

MAH deactivation

$$RO + MAH_{mon} \xrightarrow{k_{desrc}} XMAH \quad (4)$$

***β*-scission**

$$PP_n + RO \xrightarrow{k_{escpp}} PP_{n-s} + RPP_s \quad (5)$$

$$COP_n + RO \xrightarrow{k_{esccop}} COP_{n-s} + RCOP_s \quad (6)$$

$$COP_n + RO \xrightarrow{k_{esccop}} PP_{n-s} + RCOP_s \quad (7)$$

$$COP_n + RO \xrightarrow{k_{esccop}} COP_{n-s} + RPP_s \quad (8)$$

Grafting

$$RPP_n + MAH_{mon} \xrightarrow{k_{injpp}} RCOP_n^{MAH,1} \quad (9)$$

$$RCOP_n + MAH_{mon} \xrightarrow{k_{injcop}} RCOP_n^{MAH,1} \quad (10)$$

Propagation

$$RMAH_n + MAH_{mon} \xrightarrow{k_{pmah}} RMAH_{n+1} \quad (11)$$

$$RCOP_n^{MAH,m} + MAH_{mon} \xrightarrow{k_{pmah}} RCOP_n^{MAH,m+1} \quad (12)$$

Transfer to polymer

$$RPP_n + PP_s \xrightarrow{k_{tr}} PP_n + RPP_{s-t} + PP_t \quad (13)$$

$$RPP_n + COP_s \xrightarrow{k_{tr}} PP_n + COP_{s-t} + RCOP_t \quad (14)$$

$$RPP_n + COP_s \xrightarrow{k_{tr}} PP_n + PP_{s-t} + RCOP_t \quad (15)$$

$$RPP_n + COP_s \xrightarrow{k_{tr}} PP_n + COP_{s-t} + RPP_t \quad (16)$$

This article is protected by copyright. All rights reserved.

15213919, ja, Downloaded from https://onlinelibrary.wiley.com/doi/10.1002/mats.202300018 by MARIANO ASTEASUAIN - CONICET Consejo Nacional de Investigaciones , Wiley Online Library on [02/06/2023]. See the Terms and Conditions (https://onlinelibrary.wiley.com/terms-and-conditions) on Wiley Online Library for rules of use; OA articles are governed by the applicable Creative Commons License

Accepted Article

$$RCOP_n + PP_s \xrightarrow{k_{tr}} COP_n + RPP_{s-t} + PP_t \quad (17)$$

$$RCOP_n + COP_s \xrightarrow{k_{tr}} COP_n + COP_{s-t} + RCOP_t \quad (18)$$

$$RCOP_n + COP_s \xrightarrow{k_{tr}} COP_n + PP_{s-t} + RCOP_t \quad (19)$$

$$RCOP_n + COP_s \xrightarrow{k_{tr}} COP_n + COP_{s-t} + RPP_t \quad (20)$$

Termination by combination

$$RPP_n + RCOP_m \xrightarrow{k_{tcppcop}} COP_{n+m} \quad (21)$$

$$RPP_n + RMA_m \xrightarrow{k_{tcppma}} COP_n \quad (22)$$

$$RPP_n + RCOP_m^{MAH,s} \xrightarrow{k_{tcppmah}} COP_{n+m} \quad (23)$$

Termination by disproportionation

$$RPP_n + RPP_n \xrightarrow{k_{tdpppp}} PP_n + PP_n \quad (24)$$

$$RPP_n + RCOP_m \xrightarrow{k_{tdppcop}} PP_n + COP_m \quad (25)$$

$$RCOP_n + RCOP_m \xrightarrow{k_{tdcopcop}} COP_n + COP_m \quad (26)$$

$$RCOP_n + RMAH_m \xrightarrow{k_{tdcopmah}} COP_n + TMAH_m \quad (27)$$

$$RCOP_n + RCOP_m^{MAH,s} \xrightarrow{k_{tdcopmah}} COP_n + COP_m \quad (28)$$

In the above equations, PO is an unreacted peroxide, RO a peroxide radical, and MAH_{mon} the MAH monomer; $XMAH$ and XRO are deactivated MAH and peroxide molecules, respectively; $RMAH_n$ is an activated MAH chain with *n* MAH units, PPn a dead PP chain with *n* propylene units, RPP_n a PP end-chain radical with n propylene units, and COP_n is a copolymer chain with n propylene units; $RCOP_n$ is an end-chain copolymer radical with n propylene units and the radical site in a propylene unit, and $RCOP_n^{MAH,m}$ is a copolymer radical with n propylene units and the radical site at the end of a grafted MAH chain of length m; $\mathrm{TMAH_n}$ is a MAH chain of length n. Please note that reaction (4) is a simplified version of the generation of inactive species starting from peroxide radicals and MAH, through a dismutation intermediate step.[17, 29] Note that reactions (6)-(8) correspond to the same reactants resulting in different products depending on the position of the grafted MAH after the β-scission, as

This article is protected by copyright. All rights reserved.

15213919, ja, Downloaded from https://onlinelibrary.wiley.com/doi/10.1002/mats.202300018 by MARIANO ASTEASUAIN - CONICET Consejo Nacional de Investigaciones , Wiley Online Library on [02/06/2023]. See the Terms and Conditions (https://onlinelibrary.wiley.com/terms-and-conditions) on Wiley Online Library for rules of use; OA articles are governed by the applicable Creative Commons License

Accepted Article

Figure 1 illustrates. Something similar happens in reactions (14)–(16) and (18)–(20). To simplify matters, all COP_n molecules in the reaction presented before are identified with the same name. However, the model retains all the information regarding the number, length, and location of the grafted sites. Furthermore, the model can distinguish between COP_n molecules that have structural differences, such as those resulting from reaction (23).

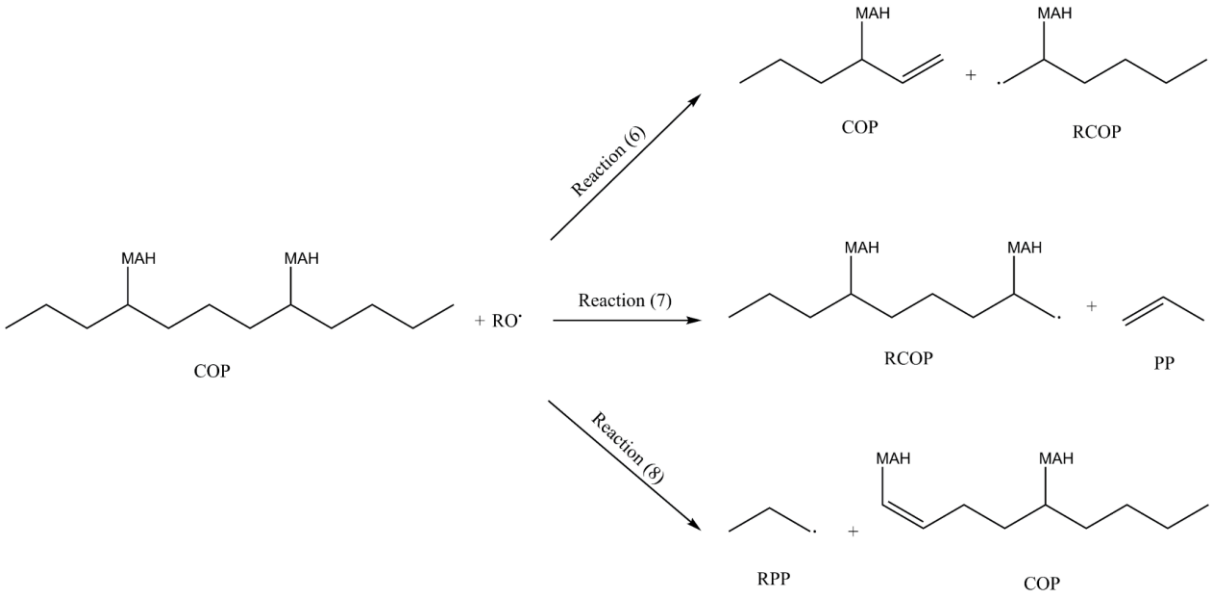


Figure 1. Possible reaction paths for the *β*-scission of COP_n molecules.

The *DG* is defined as follows:

$$DG = \frac{\left(\sum_{n=1}^{\infty}\sum_{m=1}^{\infty}\sum_{\kappa_m^*=1}^{\infty} m\kappa_m^*\left(COP_n^{\kappa_m^*} + RCOP_n^{\kappa_m^*} + RCOP_n^{MAH,\kappa_m^*}\right)\right)M_{MAH}}{\left(\sum_{n=1}^{\infty}\left(nPP_n + nRPP_n + n\sum_{m=1}^{\infty}\sum_{\kappa_m^*=1}^{\infty}\left(COP_n^{\kappa_m^*} + RCOP_n^{\kappa_m^*} + RCOP_n^{MAH,\kappa_m^*}\right)\right)\right)M_P} 100 \quad (29)$$
$$+\left(\sum_{n=1}^{\infty}\sum_{m=1}^{\infty}\sum_{\kappa_m^*=1}^{\infty} m\kappa_m^*\left(COP_n^{\kappa_m^*} + RCOP_n^{\kappa_m^*} + RCOP_n^{MAH,\kappa_m^*}\right)\right)M_{MAH}$$

In the above equation, M_{MAH} and M_P are the molecular weights of MAH and propylene, respectively. Additionally, the symbol and superscript κ_m^* stands for the number of grafted chains of length *m* in the corresponding polymer chain. It is worth noting that the model registers the position and length of every MAH graft in every polymer chain, although, for the sake of simplicity, only some of these features are made explicit in the notation as required for each particular case.

The number fraction of chains with κ-grafts (*ANGC*(κ)) is calculated as follows:

This article is protected by copyright. All rights reserved.

15213919, ja, Downloaded from https://onlinelibrary.wiley.com/doi/10.1002/mats.202300018 by MARIANO ASTEASUAIN - CONICET Consejo Nacional de Investigaciones , Wiley Online Library on [02/06/2023]. See the Terms and Conditions (https://onlinelibrary.wiley.com/terms-and-conditions) on Wiley Online Library for rules of use; OA articles are governed by the applicable Creative Commons License

Accepted Article

$$ANGC(\kappa)=\begin{cases}\dfrac{\sum_{n=1}^{\infty}\left(PP_n+RPP_n+COP_n^{\kappa}+RCOP_n^{\kappa}+RCOP_n^{MAH,\kappa}\right)}{\sum_{n=1}^{\infty}\left(PP_n+RPP_n+\sum_{\nu=1}^{\infty}\left(COP_n^{\nu}+RCOP_n^{\nu}+RCOP_n^{MAH,\nu}\right)\right)} & \kappa=0\\ \dfrac{\sum_{n=1}^{\infty}\left(COP_n^{\kappa}+RCOP_n^{\kappa}+RCOP_n^{MAH,\kappa}\right)}{\sum_{n=1}^{\infty}\left(PP_n+RPP_n+\sum_{\nu=1}^{\infty}\left(COP_n^{\nu}+RCOP_n^{\nu}+RCOP_n^{MAH,\nu}\right)\right)} & \kappa>0\end{cases} \tag{30}$$

where superscripts κ or υ stand for the number of grafts of any length in the corresponding chain.

Finally, the graft chain length distribution (*GCLD*) is computed as follows:

$$GCLD(m)=\begin{cases}\dfrac{\sum_{n=1}^{\infty}\sum_{\kappa_m^*=1}^{\infty}\left(COP_n^{\kappa_m^*}+RCOP_n^{\kappa_m^*}+RCOP_n^{MAH,\kappa_m^*}\right)}{\sum_{n=1}^{\infty}\sum_{i=1}^{\infty}\sum_{\kappa_i^*=1}^{\infty}\left(COP_n^{\kappa_i^*}+RCOP_n^{\kappa_i^*}+RCOP_n^{MAH,\kappa_i^*}\right)}\end{cases} \tag{31}$$

where *m* is the length of the MAH graft.

3. Monte Carlo Simulation

The Gillespie algorithm[52] was used to develop the MC model considering a spatially homogeneous reaction system. Reactions were assumed to occur discretely over a random reaction channel within a time interval τ. The determination of how long the time interval is and which reaction occurs is based on the following relationships:

$$\sum_{\lambda=1}^{\delta-1}P_\lambda<r_1\le\sum_{\lambda=1}^{\delta}P_\lambda \tag{32}$$

$$\tau=\left(\frac{1}{a_0}\right)\ln\left(\frac{1}{r_2}\right) \tag{33}$$

where r_1 and r_2 are random numbers between zero and one, δ is the selected reaction channel, P_λ is the reaction rate probability of reaction λ, calculated as:

$$P_\lambda=\frac{a_\lambda}{a_0} \tag{34}$$

and a_0 is the sum of all of the reaction rates:

This article is protected by copyright. All rights reserved.

15213919, ja, Downloaded from https://onlinelibrary.wiley.com/doi/10.1002/mats.202300018 by MARIANO ASTEASUAIN - CONICET Consejo Nacional de Investigaciones , Wiley Online Library on [02/06/2023]. See the Terms and Conditions (https://onlinelibrary.wiley.com/terms-and-conditions) on Wiley Online Library for rules of use; OA articles are governed by the applicable Creative Commons License

Accepted Article

$$a_0 = \sum_{\lambda} a_{\lambda} \tag{35}$$

According to the reaction scheme presented before, we can list the reaction rates as follows:

$$a_1 = k_d^{MC} n_{PO} \tag{36}$$

$$a_2 = k_{desro}^{MC} n_{RO} \left(n_{RO} - 1 \right) \tag{37}$$

$$a_3 = k_{imah}^{MC} n_{RO} n_{MAH} \tag{38}$$

$$a_4 = k_{desrc}^{MC} n_{RO} n_{MAH} \tag{39}$$

$$a_5 = k_{escpp}^{MC} n_{RO} u_{PP} \tag{40}$$

$$a_{6-8} = k_{esccop}^{MC} n_{RO} u_{COP} \tag{41}$$

$$a_9 = k_{injpp}^{MC} n_{RPP} n_{MAH} \tag{42}$$

$$a_{10} = k_{injcop}^{MC} n_{RCOP} n_{MAH} \tag{43}$$

$$a_{11} = k_{pmah}^{MC} n_{MAH} n_{RMAH} \tag{44}$$

$$a_{12} = k_{pmah}^{MC} n_{MAH} n_{RCOPMAH} \tag{45}$$

$$a_{13} = k_{tr}^{MC} n_{RPP} u_{PP} \tag{46}$$

$$a_{14-16} = k_{tr}^{MC} n_{RPP} u_{COP} \tag{47}$$

$$a_{17} = k_{tr}^{MC} n_{RCOP} u_{PP} \tag{48}$$

$$a_{18-20} = k_{tr}^{MC} n_{RCOP} u_{COP} \tag{49}$$

$$a_{21} = k_{tcppcop}^{MC} n_{RPP} n_{RCOP} \tag{50}$$

$$a_{22} = k_{tcppmah}^{MC} n_{RPP} n_{RMAH} \tag{51}$$

$$a_{23} = k_{tcppmah}^{MA} n_{RPP} n_{RCOPMAH} \tag{52}$$

This article is protected by copyright. All rights reserved.

15213919, ja, Downloaded from https://onlinelibrary.wiley.com/doi/10.1002/mats.202300018 by MARIANO ASTEASUAIN - CONICET Consejo Nacional de Investigaciones , Wiley Online Library on [02/06/2023]. See the Terms and Conditions (https://onlinelibrary.wiley.com/terms-and-conditions) on Wiley Online Library for rules of use; OA articles are governed by the applicable Creative Commons License

Accepted Article

$$a_{24} = k_{tdpppp}^{MC} n_{RPP}(n_{RPP} - 1) \tag{53}$$

$$a_{25} = k_{tdppcop}^{MC} n_{RPP} n_{RCOP} \tag{54}$$

$$a_{26} = k_{tdcopcop}^{MC} n_{RCOP}(n_{RCOP} - 1) \tag{55}$$

$$a_{27} = k_{tdcopmah}^{MC} n_{RCOP} n_{RMAH} \tag{56}$$

$$a_{28} = k_{tdcopmah}^{MC} n_{RCOP} n_{RCOPMAH} \tag{57}$$

where n is the total number of molecular species and u is the sum of all valid reaction sites of these species. To use the MC algorithm, the original macroscopic kinetic constants (k) must be converted to microscopic ones (k^{MC}). The conversion can be achieved using the following relations:

1st order reactions

$$k_i^{MC} = k_i \tag{58}$$

2nd order reactions

$$k_i^{MC} = \frac{k_i}{VN_A} \tag{59}$$

where V is the reaction volume and N_A is Avogadro's number. Initial values of the macroscopic kinetic constants, obtained from the literature[53] and previous work by our group,[54] are shown in **Table 2**.

Table 2. Macroscopic kinetic rate constants.

k_d [s^{-1}]	9.3×10^{-3}	k_{desro} [L mol^{-1} s^{-1}]	1.53×10^{-2}
k_{imah} [L mol^{-1} s^{-1}]	1.09×10^{-2}	k_{desrc} [L mol^{-1} s^{-1}]	1.58×10^{-2}
k_{escpp} [L mol^{-1} s^{-1}]	4.09×10^{-4}	k_{esccop} [L mol^{-1} s^{-1}]	2.04×10^{1}
k_{injpp} [L mol^{-1} s^{-1}]	1×10^{-6}	k_{injcop} [L mol^{-1} s^{-1}]	1.97×10^{-1}
k_{pmah} [L mol^{-1} s^{-1}]	7.3×10^{-1}	k_{tr} [L mol^{-1} s^{-1}]	1.45×10^{-1}
$k_{tcppcop}$ [L mol^{-1} s^{-1}]	7.54×10^{-2}	$k_{tcppmah}$ [L mol^{-1} s^{-1}]	1.11×10^{1}
k_{tdpppp} [L mol^{-1} s^{-1}]	1.45×10^{-1}	$k_{tdppcop}$ [L mol^{-1} s^{-1}]	1.45×10^{-1}
$k_{tdcopcop}$ [L mol^{-1} s^{-1}]	1.45×10^{-1}	$k_{tdcopmah}$ [L mol^{-1} s^{-1}]	4.76×10^{4}

This article is protected by copyright. All rights reserved.

15213919, ja, Downloaded from https://onlinelibrary.wiley.com/doi/10.1002/mats.202300018 by MARIANO ASTEASUAIN - CONICET Consejo Nacional de Investigaciones , Wiley Online Library on [02/06/2023]. See the Terms and Conditions (https://onlinelibrary.wiley.com/terms-and-conditions) on Wiley Online Library for rules of use; OA articles are governed by the applicable Creative Commons License

Accepted Article

The model was implemented in MATLAB®.

4. Model validation

First, a sensitivity analysis was performed to evaluate the effects of each step of the kinetic mechanism on the molecular properties of the copolymer. A number of approaches have been reported in the literature for addressing the model sensitivity to the values of its parameters, such as distribution-numerical fractionation-method of moments,[45] principal component analysis,[55] estimability analysis,[56, 57] design of experiments[58] and Sobol' indices,[59, 60] among others. In this work, an ad-hoc procedure was employed. The analysis was performed by simulating the grafting reactions of PP-A under different operating conditions, shown in **Table 3**. These conditions were chosen to give significantly different final properties. A reaction time of 2400 s was used for all cases.

Table 3. Operating conditions for the sensitivity analysis.

Simulation	Initiator [ppm]	MAH [w/w%]
Sim.I	1000	1
Sim.II	1000	3
Sim.III	1000	4.5
Sim.IV	10000	1
Sim.V	10000	4.5
Sim.VI	10000	10

In the first step of the sensitivity analysis, the average frequency of each kinetic step in the series of simulated grafting reactions was recorded using the kinetic constants listed in Table 2. Secondly, the grafting process was simulated for each initial condition given in Table 3 scaling the kinetic constants in Table 2 by a factor of 0.01, 0.1, 10, and 100. The resulting values of $\overline{M_n}$, $\overline{M_w}$, and *DG* were compared with the ones obtained using the original values of the constants in order to determine the effect of each reaction on the final copolymer properties. To quantify this effect, a performance indicator ξ was defined that represents the influence of a variation of a kinetic constant on a particular polymer property (e.g., $\overline{M_n}$) compared to the total influence of all kinetic constants on the same property. This parameter is calculated as follows:

This article is protected by copyright. All rights reserved.

15213919, ja, Downloaded from https://onlinelibrary.wiley.com/doi/10.1002/mats.202300018 by MARIANO ASTEASUAIN - CONICET Consejo Nacional de Investigaciones , Wiley Online Library on [02/06/2023]. See the Terms and Conditions (https://onlinelibrary.wiley.com/terms-and-conditions) on Wiley Online Library for rules of use; OA articles are governed by the applicable Creative Commons License

Accepted Article

$$\xi(\varphi,\psi)=\frac{\sum_{j=1}^{m}\sum_{i=1}^{n}\left|\theta_{0,j,\varphi,\psi}-\theta_{i,j,\varphi,\psi}\right|}{\sum_{k=1}^{p}\sum_{j=1}^{m}\sum_{i=1}^{n}\left|\theta_{0,j,k,\psi}-\theta_{i,j,k,\psi}\right|} \tag{60}$$

where φ stands for the property of interest, ψ is the evaluated reaction, n is the total number of multiplying factors for the analysis, m is the total number of data sets, p is the total number of kinetic constants, and θ is the numerical value of the property φ. From the model validation details, experimental data, and model formulation, n = 4, m = 6, and p = 16, respectively. A higher value of $\xi(\varphi,\psi)$ indicates a higher influence of the reaction ψ on the property φ.

The results of the sensitivity analysis were used to select the four most influential reactions, whose kinetic constants were then tuned to fit the model results to the experimental data in Table 1. The objective function of the parameter estimation problem was:

$$\varepsilon(f)=\sum_{i=1}^{m}\left(\begin{array}{l} w\left(\overline{M_n}\right)_i\left(\dfrac{\overline{M}_{n\,\exp,i}-\overline{M}_{n\,sim,i}(f)}{\overline{M}_{n\,\exp,i}}\right)^2+w\left(\overline{M_w}\right)_i\left(\dfrac{\overline{M}_{w\,\exp,i}-\overline{M}_{w\,sim,i}(f)}{\overline{M}_{w\,\exp,i}}\right)^2 \\ +w(DG)_i\left(\dfrac{DG_{\exp,i}-DG_{sim,i}(f)}{DG_{\exp,i}}\right) \\ +w(MWDc)_i\sum_{j=1}^{l_i}\left(\dfrac{MWDc_{\exp,i,j}-MWDc_{sim,i,j}(f)}{MWDc_{\exp,i,j}}\right)^2 \end{array}\right) \tag{61}$$

where f is the vector of the selected kinetic constants, exp refers to experimental data, and sim to simulated data; $MWDc_{exp/sim,i,j}$ is the experimental/simulated cumulative molecular weight distribution at the chain length *j* for the data set *i*; m is the number of data sets, l_i is the maximum chain length of the MWDc of the data set *i*, and the $w(\varphi)_i$ is the weighting factor of the property φ =$\overline{M_n}$, $\overline{M_w}$, *DG* or MWDc, for the data set *i*.

The weighting factors are calculated using the relationship presented in Equation (62) and are shown in **Table 4**:

This article is protected by copyright. All rights reserved.

15213919, ja, Downloaded from https://onlinelibrary.wiley.com/doi/10.1002/mats.202300018 by MARIANO ASTEASUAIN - CONICET Consejo Nacional de Investigaciones , Wiley Online Library on [02/06/2023]. See the Terms and Conditions (https://onlinelibrary.wiley.com/terms-and-conditions) on Wiley Online Library for rules of use; OA articles are governed by the applicable Creative Commons License

Accepted Article

$$w(\varphi)_i = \frac{\dfrac{\delta_{\varphi,i}}{\left(ME(\varphi)\right)^2}}{\displaystyle\sum_i \frac{\delta_{\varphi,i}}{\left(ME(\varphi)\right)^2}} \tag{62}$$

where $w(\varphi)_i$ is the weighting factor of the property φ in experiment i, ME(φ) is the experimental measurement error of the property φ, and $\delta_{\varphi,i}$ = 1 if the data of property φ is available in experiment i or 0 otherwise. Note that the experimental MWD is only available for experiments E. IV and E.V, and therefore the weights of the other properties are lower for these experiments than for the other ones.

Table 4. Weighting factors for the fitting problem.

Property	Experimental measurement error	$\delta_{\varphi,i}$		$w(\varphi)_i$	
		E.I-E.III	E.IV & E.V	E.I-E.III	E.IV & E.V
$\overline{M_n}$	±15%	1	1	0.09	0.06
$\overline{M_w}$	±5%	1	1	0.73	0.62
DG	±10%	1	1	0.18	0.16
MWDc	±10%	0	1	0	0.16

Given the probabilistic nature of the model, conventional optimization methods are not suitable for parameter estimation. Therefore, the Surface Response Method (SRM) was chosen, which is effective for stochastic optimization.[61, 62] This method allows the construction of approximate models, called response-surface models, between the system variables (in this case, the kinetic constants) and the response values (the objective function ε).[63, 64] In this work, a response surface model of second-order was used (Equation (63)). This model structure is frequently chosen because it usually adequately captures the behavior of the response surface, especially within a limited region of interest.[65]

$$y_i = c_0 + \sum_{j=1}^{n} c_{1j} x_{ij} + \sum_{j=1}^{n} \sum_{k=j}^{n} c_{2jk} x_{ij} x_{ik} \tag{63}$$

In Equation (63), x_{ij} are the system variables that affect the response y_i, and c_0, c_{1j}, and c_{2jk} are estimated regression coefficients. These coefficients are found using a least-squares approach. The D-

This article is protected by copyright. All rights reserved.

15213919, ja, Downloaded from https://onlinelibrary.wiley.com/doi/10.1002/mats.202300018 by MARIANO ASTEASUAIN - CONICET Consejo Nacional de Investigaciones , Wiley Online Library on [02/06/2023]. See the Terms and Conditions (https://onlinelibrary.wiley.com/terms-and-conditions) on Wiley Online Library for rules of use; OA articles are governed by the applicable Creative Commons License

Accepted Article

optimum criterion was used to construct the experimental designs because they provide a minimum variance error.[65]

The optimization procedure of the SRM used in this work is relatively straightforward and has the following steps:[61, 62]

(A) a D-optimal experimental design is created from an initial point of the system variables. In this work, a variation of ±25 % from the initial point is considered for the design factors ±1, i.e. the design factor ±1 equals ±25 % of the initial point for each system variable.

(B) response values are obtained with the MC model for each value of the system variables indicated by the experimental design formulated in step (A).

(C) using a least squares method, a response surface model is obtained by tuning the coefficients c_0, $c_{1j,}$ and c_{2jk} in Equation (63) to fit the response values calculated in step (B).

(D) the response surface model obtained in step (C) is minimized by varying the system variables.

(E) Convergence is checked by evaluating the optimum obtained in step (D) with the initial point in step (A). If the difference is less than ±10 % for each of the system variables, the algorithm ends; if not, the process is repeated from step (A) using the values of the system variables found in (D) as the initial point.

The parameter estimation problem was repeated with different initial points, observing no noticeable changes in the optimal set of the kinetic constants. The ±25 % perturbation value was selected after preliminary numerical tests: smaller values led to the same result but in a longer time, while larger values affected the convergence of the algorithm.

5. Results and Discussion

5.1. Model validation

Table 5 shows the average frequencies of the different reactions that make up the kinetic mechanism as well as the calculated values of $\xi(\varphi,\psi)$, which measure the influence of kinetic constants on particular polymer properties.

This article is protected by copyright. All rights reserved.

15213919, ja, Downloaded from https://onlinelibrary.wiley.com/doi/10.1002/mats.202300018 by MARIANO ASTEASUAIN - CONICET Consejo Nacional de Investigaciones , Wiley Online Library on [02/06/2023]. See the Terms and Conditions (https://onlinelibrary.wiley.com/terms-and-conditions) on Wiley Online Library for rules of use; OA articles are governed by the applicable Creative Commons License

Accepted Article

Table 5. Effect of changes in kinetic constants on polymer properties.

Reaction number (ψ)	Kinetic constant	Average rate of occurrence %	$\xi(\overline{M_n}, \psi)$	$\xi(\overline{M_w}, \psi)$	$\xi(DG, \psi)$
(1)	k_d	3.08	0.144	0.114	0.016
(2)	k_{desro}	0.80	0.131	0.099	0.016
(3)	k_{imah}	0.77	0.059	0.050	0.151
(4)	k_{desrc}	1.11	0.152	0.111	0.017
(5)	k_{escpp}	6.72	**0.151**	**0.146**	0.043
(6)-(8)	k_{esccop}	1.40	0.006	0.017	0.006
(9)	k_{injpp}	1×10^{-4}	0.002	0.006	0.002
(10)	k_{injcop}	0.03	0.061	0.020	**0.149**
(11)	k_{pmah}	82.14	0.001	0.002	**0.077**
(12)	k_{pmah}	1.25	0.004	0.007	**0.137**
(13)	k_{tr}	0.51	0.109	0.138	0.001
(14)-(16)	k_{tr}	4×10^{-6}	0.001	0.003	0.004
(17)	k_{tr}	3×10^{-4}	0.004	0.015	0.006
(18)-(20)	k_{tr}	0	0	0	0
(21)	$k_{tcppcop}$	5×10^{-4}	0.002	0.007	0.002
(22)	$k_{tcppmah}$	0.16	0.058	0.026	0.214
(23)	$k_{tcppmah}$	0.01	0.007	0.001	0.003
(24)	k_{tdpppp}	1.39	0.045	**0.207**	0.011
(25)	$k_{tdppcop}$	9×10^{-4}	0.002	0.010	0.001
(26)	$k_{tdcopcop}$	0	0	0	0
(27)	$k_{tdcopmah}$	0.81	0.058	0.014	0.123
(28)	$k_{tdcopmah}$	0.02	0.003	0.007	0.025

Homopolymerization of MAH (reaction (11)) occurs most frequently, accounting for 82 % of the total number of reactions that took place in the simulated experiments. In contrast, reactions (14)-(16) are very unlikely. Transfer from copolymer radicals to dead copolymers (reactions (18)-(20)) and

This article is protected by copyright. All rights reserved.

15213919, ja, Downloaded from https://onlinelibrary.wiley.com/doi/10.1002/mats.202300018 by MARIANO ASTEASUAIN - CONICET Consejo Nacional de Investigaciones , Wiley Online Library on [02/06/2023]. See the Terms and Conditions (https://onlinelibrary.wiley.com/terms-and-conditions) on Wiley Online Library for rules of use; OA articles are governed by the applicable Creative Commons License

Accepted Article

termination by disproportionation between copolymer radicals (reaction (26)) do not occur. Transfer to polymer reactions (reactions (13)-(20)) make a difference only when both reactants are PP chains (reaction (13)), both because of their frequency and of their effect on the polymer properties. Since all transfer to polymer reactions have the same kinetic constant, this can be explained by the combination of a small population of copolymer molecules and a predominance of other reactions in which copolymers serve as reactants. Hence, reactions (14)-(20) can be neglected due to their low frequency and impact on polymer properties. All other reactions affect at least one polymer property and occur at a reasonable rate.

Although several reactions affect significantly the polymer properties, only four of them were chosen to be fitted because of the limited number of available experimental points. The four kinetic selected kinetic constants were: k_{escpp}, k_{injcop}, k_{pmah}, and k_{tdpppp}. The constant k_{escpp} is the most influential on $\overline{M_n}$ and the second most influential on $\overline{M_w}$, k_{injcop} is the second most influential on *DG*, k_{pmah}, adding the contributions of reactions (11) and (12), has the highest influence on *DG* together with $k_{tcppmah}$ but with a higher rate of occurrence than the latter, and k_{tdpppp} has the highest influence on $\overline{M_w}$. Initiator-induced reactions are frequent and also affect polymer properties, but they were not selected because values available in the literature are generally well accepted.[53] It should be noted that the ranking of most significant kinetic steps may be different for other grafting systems.[55]

The final values of the estimated kinetic constants obtained using the SRM are given in **Table 6**. The response surfaces corresponding to the minimum point are shown in **Figure 2**. It can be noted that the response surfaces are centered very near to the (0,0) which is the coordinate required for a minimum point, presenting a reasonable error margin.

Table 6. Final values of the estimated kinetic constants.

Reaction number	Kinetic constant	Final value [L mol^{-1} s^{-1}]
(5)	k_{escpp}	5.28×10^{-4}
(10)	k_{injcop}	5.2×10^{0}
(11),(12)	k_{pmah}	2.31×10^{1}
(24)	k_{tdpppp}	5.55×10^{-1}

This article is protected by copyright. All rights reserved.

15213919, ja, Downloaded from https://onlinelibrary.wiley.com/doi/10.1002/mats.202300018 by MARIANO ASTEASUAIN - CONICET Consejo Nacional de Investigaciones , Wiley Online Library on [02/06/2023]. See the Terms and Conditions (https://onlinelibrary.wiley.com/terms-and-conditions) on Wiley Online Library for rules of use; OA articles are governed by the applicable Creative Commons License

Accepted Article

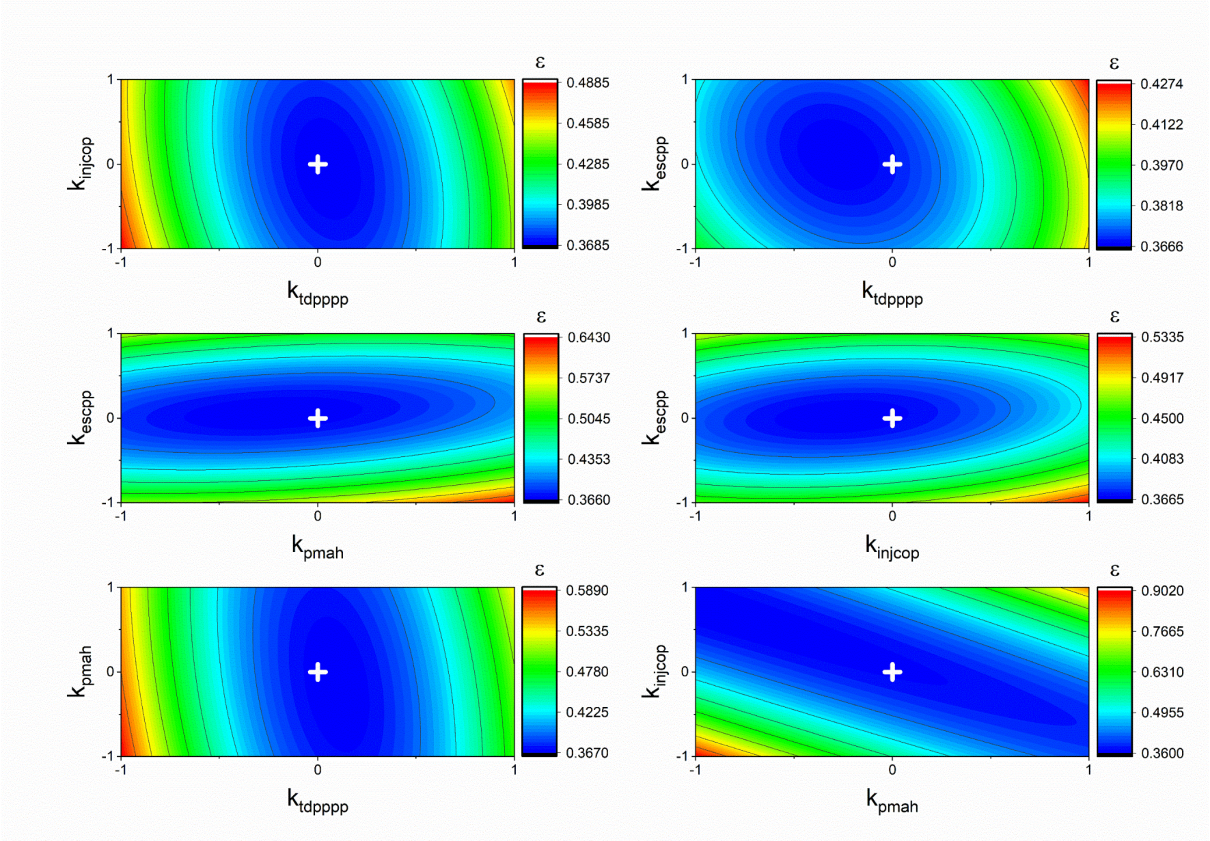


Figure 2. Response surfaces corresponding to the optimal point

Figure 3 and **Figure 4** compare simulated and experimental data for $\overline{M_n}$, $\overline{M_w}$, and *DG*. There is a good degree of agreement. The average relative errors for $\overline{M_n}$, $\overline{M_w}$, and *DG* are 21.1 %, 5.3 %, and 7.9 %, respectively. These values are consistent with the experimental errors reported in Table 4, although the one for $\overline{M_n}$ is slightly higher.

Figure 5 and **Figure 6** show the experimental and simulated MWD and MWDc for experiments E.IV and E.V. Both the cumulative MWD, which was used to fit the kinetic constants, and the MWD of the modified resins are depicted, along with the MWD of the virgin PP. The curves for the simulated distributions have been smoothed using splines to minimize the numerical noise inherent to MC simulations. Overall, the agreement between the simulated and experimental MWDs is good. There are small discrepancies near the peak of the distributions, but they are not very significant.

This article is protected by copyright. All rights reserved.

15213919, ja, Downloaded from https://onlinelibrary.wiley.com/doi/10.1002/mats.202300018 by MARIANO ASTEASUAIN - CONICET Consejo Nacional de Investigaciones , Wiley Online Library on [02/06/2023]. See the Terms and Conditions (https://onlinelibrary.wiley.com/terms-and-conditions) on Wiley Online Library for rules of use; OA articles are governed by the applicable Creative Commons License

Accepted Article

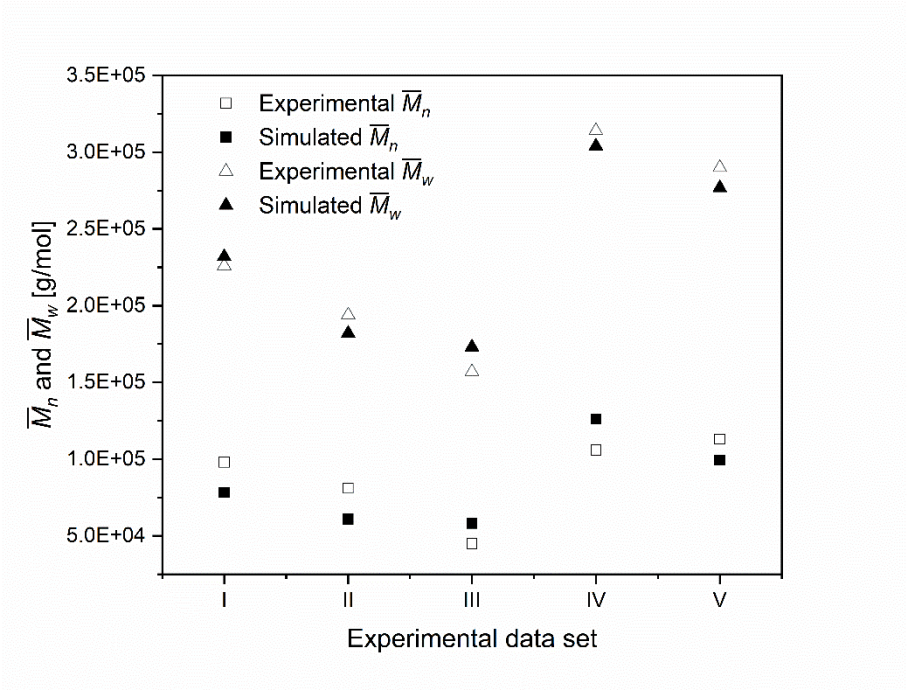


Figure 3. Experimental and simulated $\overline{M_n}$ and $\overline{M_w}$.

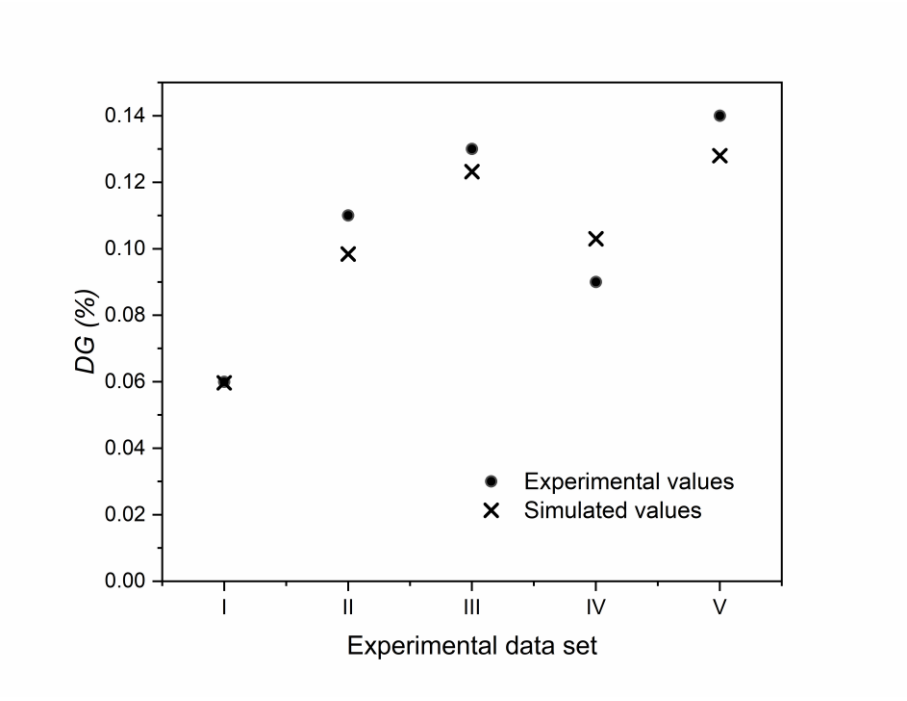


Figure 4. Experimental and simulated *DG*.

This article is protected by copyright. All rights reserved.

15213919, ja, Downloaded from https://onlinelibrary.wiley.com/doi/10.1002/mats.202300018 by MARIANO ASTEASUAIN - CONICET Consejo Nacional de Investigaciones , Wiley Online Library on [02/06/2023]. See the Terms and Conditions (https://onlinelibrary.wiley.com/terms-and-conditions) on Wiley Online Library for rules of use; OA articles are governed by the applicable Creative Commons License

Accepted Article

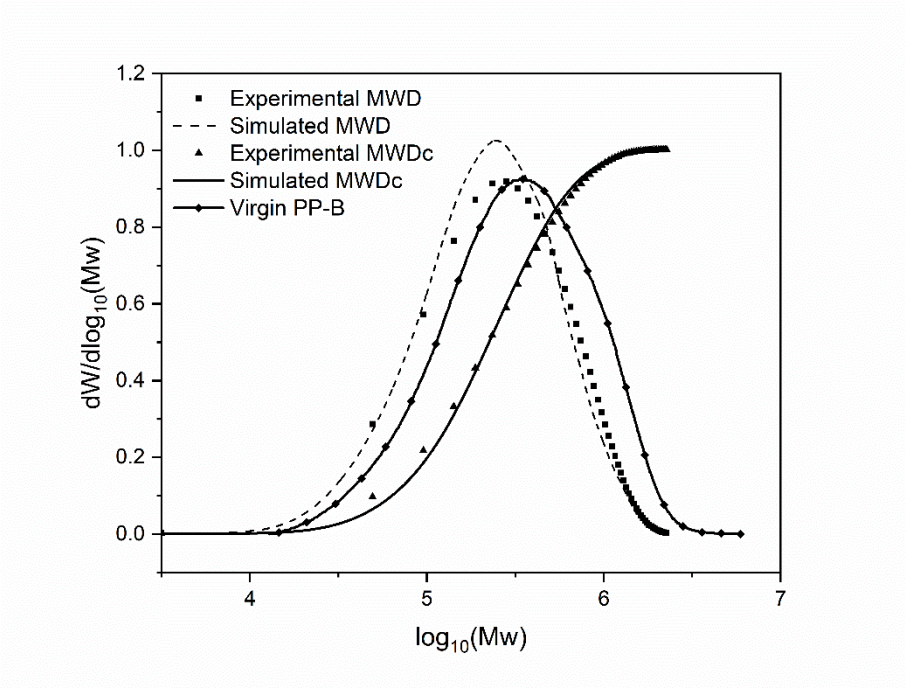


Figure 5. Experimental and simulated MWD and MWDc for E.IV. PO 250 ppm, MA 1% w/w, t=15 min.

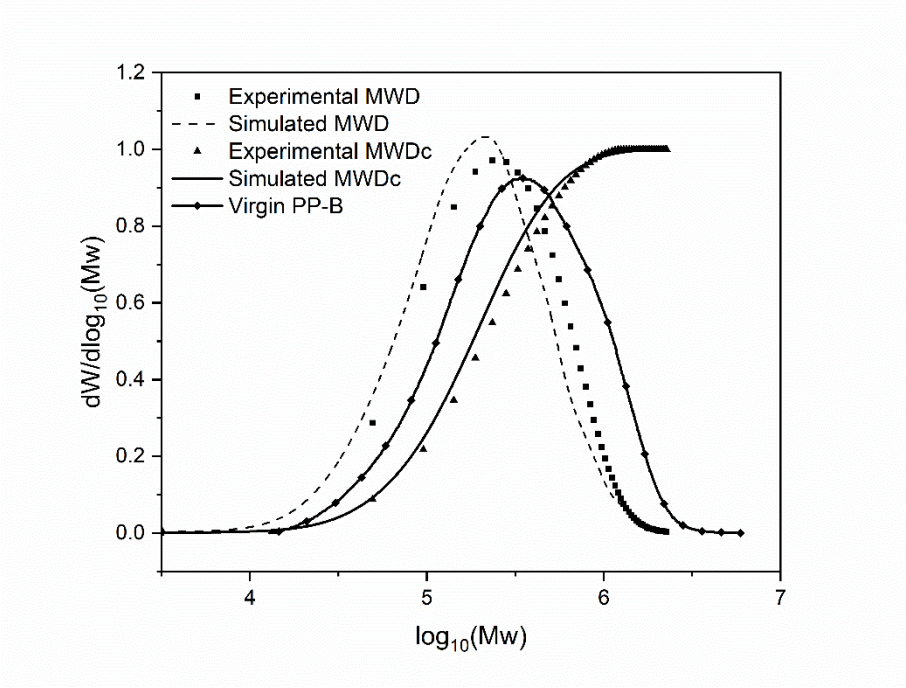


Figure 6. Experimental and simulated MWD and MWDc for E.V. PO 500 ppm, MA 1% w/w, t=15 min.

5.2. Effect of the process variables on the polymer properties

The MC model was used to investigate the influence of the initial concentrations of PO and MAH and of the reaction time on the polymer properties. **Table 7** shows the values of the process variables

This article is protected by copyright. All rights reserved.

15213919, ja, Downloaded from https://onlinelibrary.wiley.com/doi/10.1002/mats.202300018 by MARIANO ASTEASUAIN - CONICET Consejo Nacional de Investigaciones , Wiley Online Library on [02/06/2023]. See the Terms and Conditions (https://onlinelibrary.wiley.com/terms-and-conditions) on Wiley Online Library for rules of use; OA articles are governed by the applicable Creative Commons License

Accepted Article

considered in this analysis. One variable was modified at a time, keeping the other two fixed at the values marked with an asterisk.

Table 7. Initial values for the variables used for sensitivity analysis.

PO [ppm]	MAH [w/w %]	t [min]
250	0.5	5
375	0.75	15*
500*	1*	22.5
625	1.25	33
750	1.5	40

The effects of the initial concentrations of PO and MAH on $\overline{M_n}$, $\overline{M_w}$ and *DG* are shown in **Figure 7**, **Figure 8** and **Figure 9**. It can be seen that as the concentration of PO increases, $\overline{M_n}$ decreases (Figure 7a). A higher concentration of PO increases the frequency of the β-scission reactions, resulting in a larger population of shorter chains. On the other hand, an increase in the concentration of MAH has a minor effect on $\overline{M_n}$ (Figure 7b). Additionally, Figure 7c shows that increasing the reaction time beyond 15 minutes has a negligible effect on $\overline{M_n}$, presumably because all RO molecules have already been consumed. Regarding $\overline{M_w}$ (Figure 8), a similar trend is observed. The only significant difference is found in the influence of MAH, which causes a slightly higher increase in $\overline{M_w}$. Regarding *DG*, it can be seen that increasing the initial PO concentration causes a minor increment in the grafting values, whereas the initial MAH concentration has a significant effect. As with the other cases, *DG* values tend to stabilize after 15 minutes of reaction time. These results are in agreement with other published works.[7, 28, 32, 33]

This article is protected by copyright. All rights reserved.

15213919, ja, Downloaded from https://onlinelibrary.wiley.com/doi/10.1002/mats.202300018 by MARIANO ASTEASUAIN - CONICET Consejo Nacional de Investigaciones , Wiley Online Library on [02/06/2023]. See the Terms and Conditions (https://onlinelibrary.wiley.com/terms-and-conditions) on Wiley Online Library for rules of use; OA articles are governed by the applicable Creative Commons License

Accepted Article

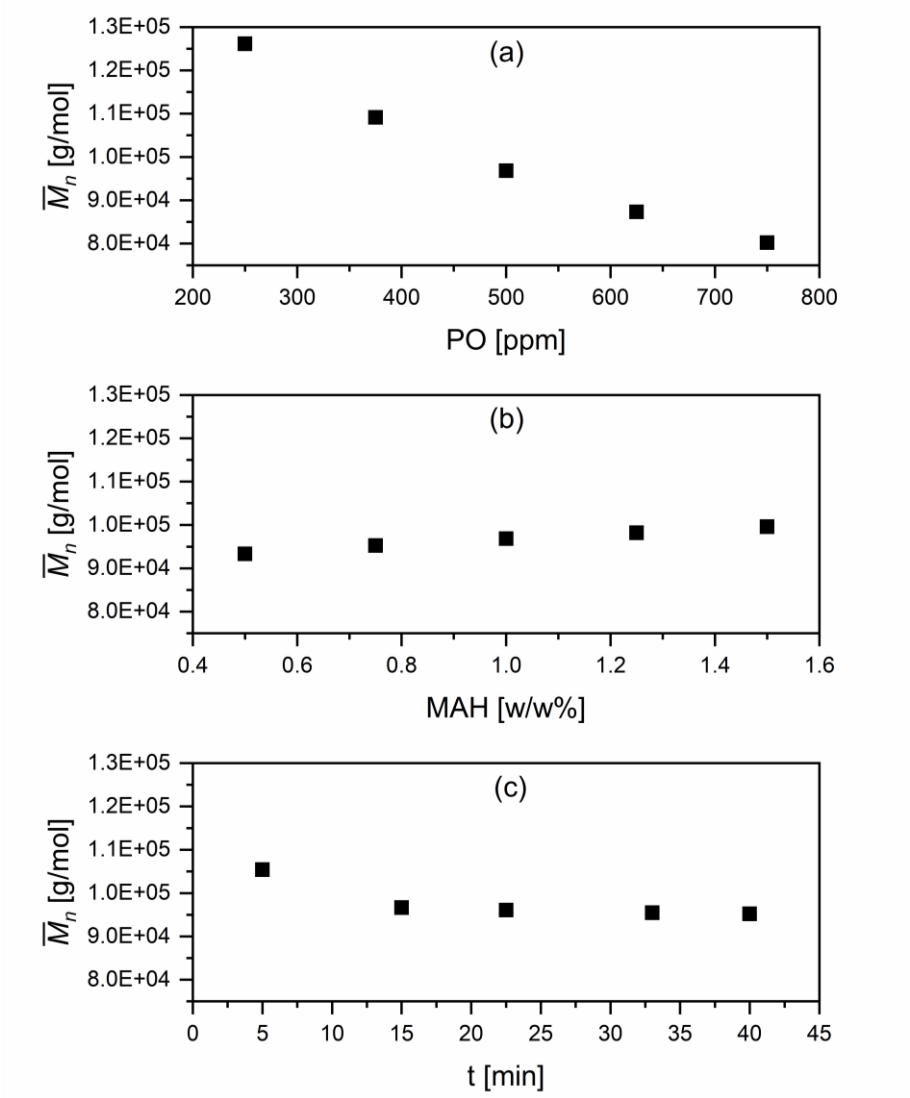


Figure 7. Effect of operating variables on $\overline{M_n}$. (a) MAH 1 w/w%, t=15 min; (b) PO 500 ppm, t=15 min; (c) PO 500 ppm, MAH 1 w/w%.

This article is protected by copyright. All rights reserved.

15213919, ja, Downloaded from https://onlinelibrary.wiley.com/doi/10.1002/mats.202300018 by MARIANO ASTEASUAIN - CONICET Consejo Nacional de Investigaciones , Wiley Online Library on [02/06/2023]. See the Terms and Conditions (https://onlinelibrary.wiley.com/terms-and-conditions) on Wiley Online Library for rules of use; OA articles are governed by the applicable Creative Commons License

Accepted Article

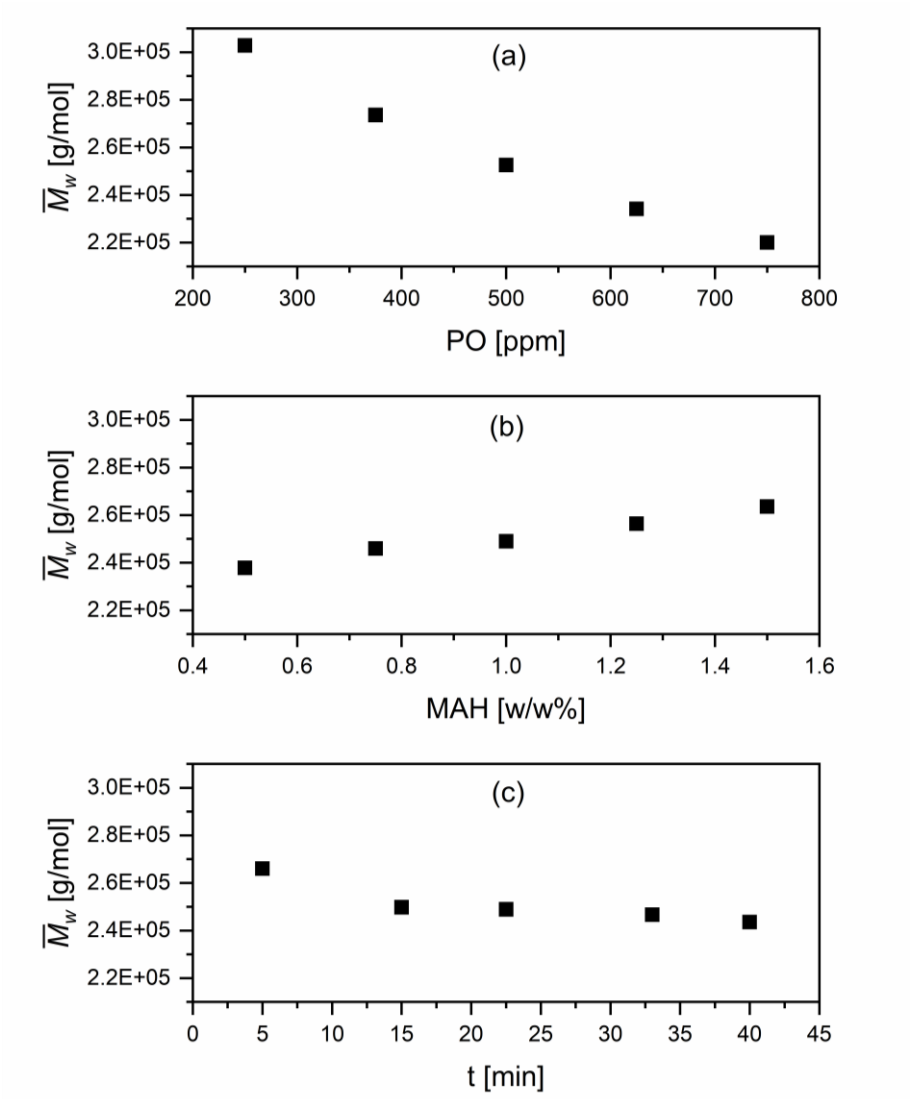


Figure 8. Effect of operating variables on $\overline{M_w}$. (a) MAH 1 w/w%, t=15 min; (b) PO 500 ppm, t=15 min; (c) PO 500 ppm, MAH 1 w/w%.

This article is protected by copyright. All rights reserved.

15213919, ja, Downloaded from https://onlinelibrary.wiley.com/doi/10.1002/mats.202300018 by MARIANO ASTEASUAIN - CONICET Consejo Nacional de Investigaciones , Wiley Online Library on [02/06/2023]. See the Terms and Conditions (https://onlinelibrary.wiley.com/terms-and-conditions) on Wiley Online Library for rules of use; OA articles are governed by the applicable Creative Commons License

Accepted Article

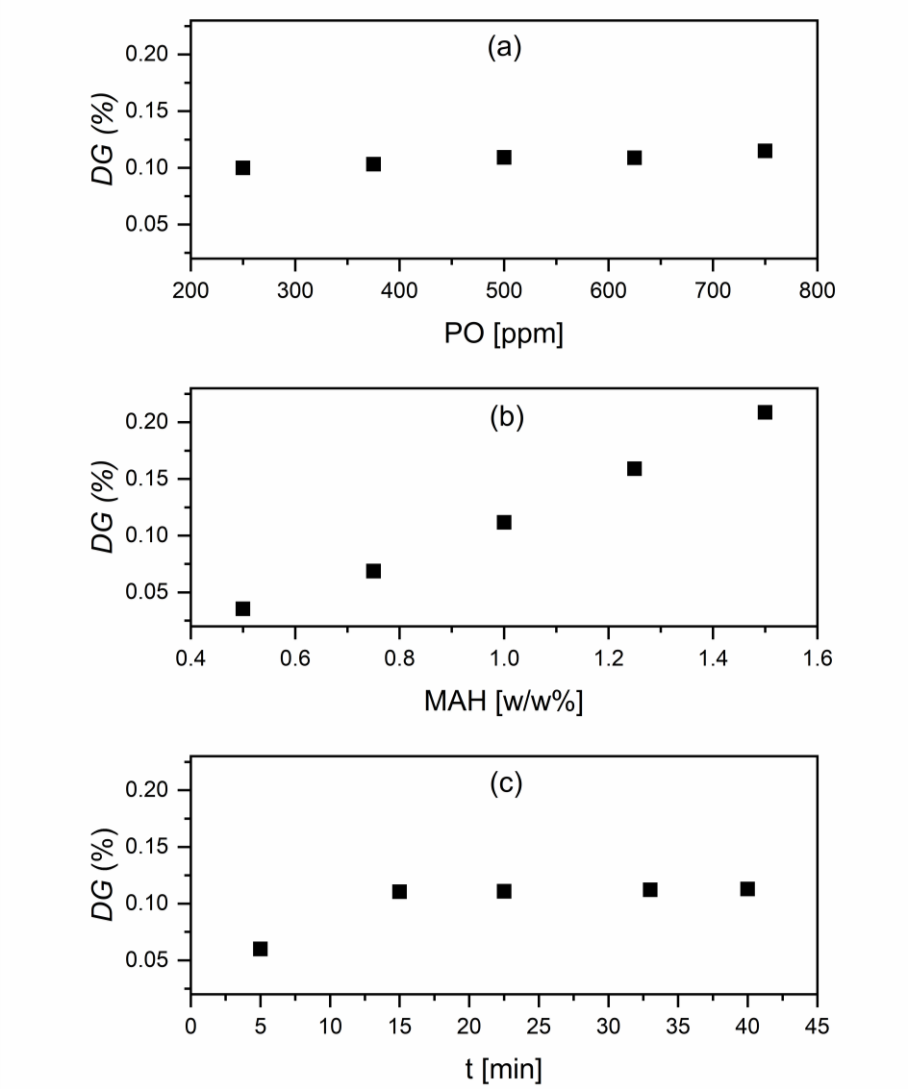


Figure 9. Effect of operating variables on *DG*. (a) MAH 1 w/w%, t=15 min; (b) PO 500 ppm, t=15 min; (c) PO 500 ppm, MAH 1 w/w%.

The impact of the operating variables on *GCLD* is shown in **Figure 10**, **Figure 11**, and **Figure 12**. When the initial concentration of PO increases, the concentration of short-grafted chains also increases. Conversely, an increase in the initial concentration of MAH generates higher concentrations of longer grafted chains, something that could be attributed to a higher incidence of homopolymerization reactions. The reaction time appears to have a negligible effect on the length of the grafted chains. Additionally, the results show that, on average, 25 % of the grafts are less than 6 units long, while 50% are less than 15 units long. Only 5% of grafts are longer than 93 units.

This article is protected by copyright. All rights reserved.

15213919, ja, Downloaded from https://onlinelibrary.wiley.com/doi/10.1002/mats.202300018 by MARIANO ASTEASUAIN - CONICET Consejo Nacional de Investigaciones , Wiley Online Library on [02/06/2023]. See the Terms and Conditions (https://onlinelibrary.wiley.com/terms-and-conditions) on Wiley Online Library for rules of use; OA articles are governed by the applicable Creative Commons License

Accepted Article

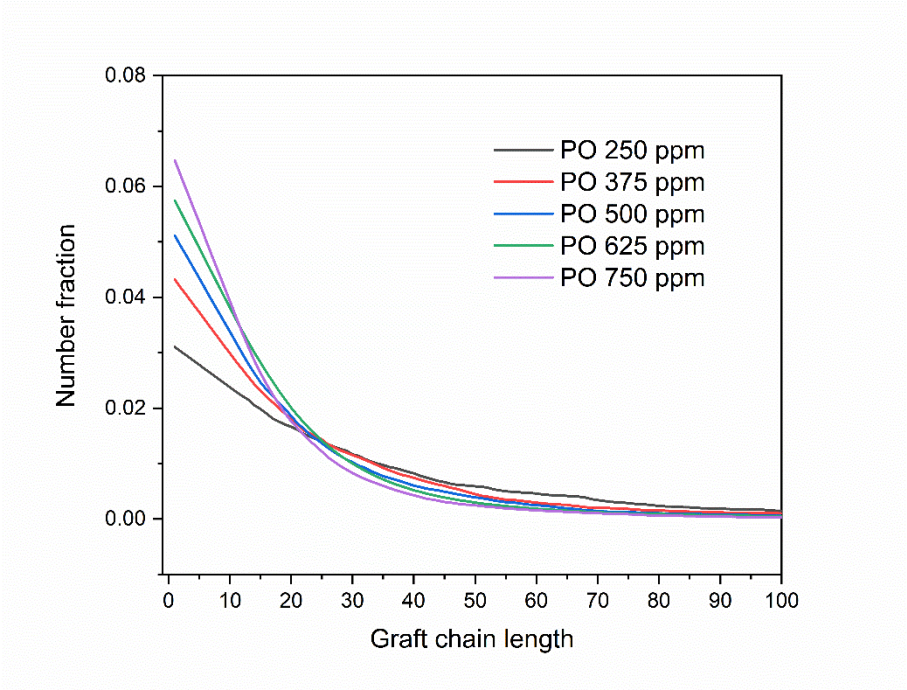


Figure 10. Graft chain length distributions at different PO concentrations. MAH 1 w/w%, t=15 min.

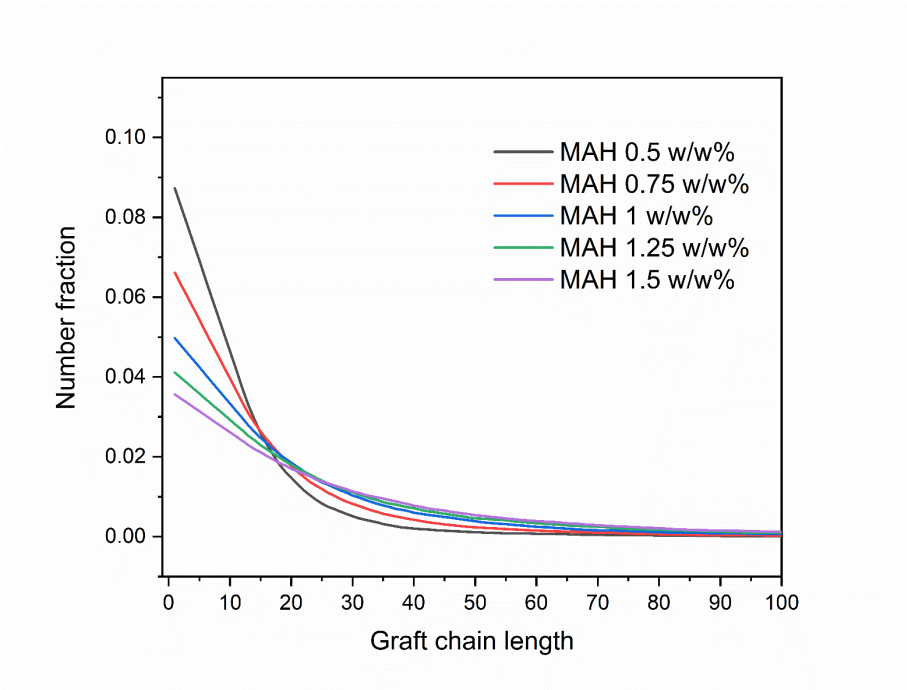


Figure 11. Graft chain length distributions at different MAH concentrations. PO 500 ppm, t=15 min.

This article is protected by copyright. All rights reserved.

15213919, ja, Downloaded from https://onlinelibrary.wiley.com/doi/10.1002/mats.202300018 by MARIANO ASTEASUAIN - CONICET Consejo Nacional de Investigaciones , Wiley Online Library on [02/06/2023]. See the Terms and Conditions (https://onlinelibrary.wiley.com/terms-and-conditions) on Wiley Online Library for rules of use; OA articles are governed by the applicable Creative Commons License

Accepted Article

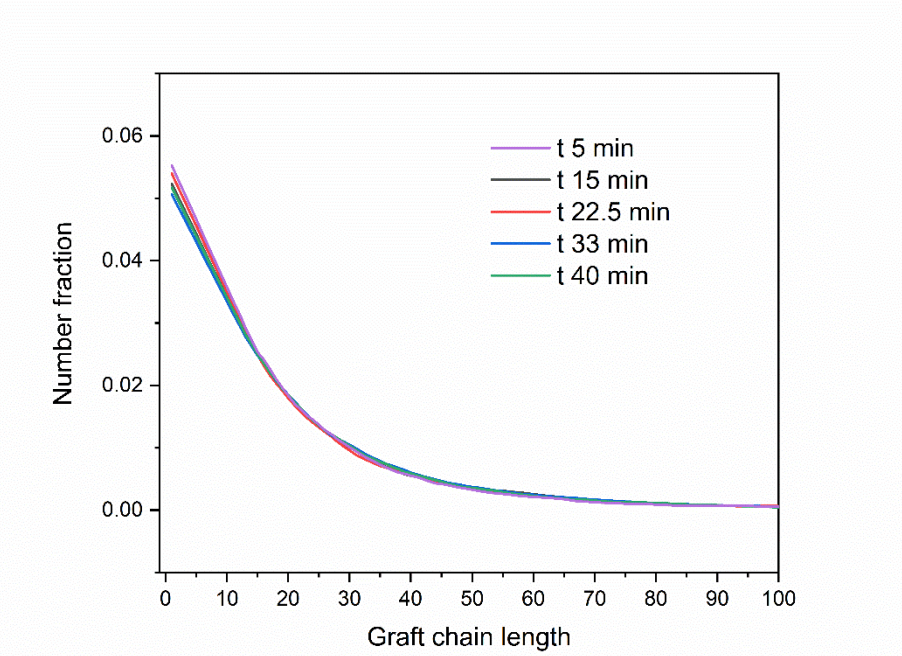


Figure 12. Graft chain length distributions at different final reaction times. PO 500 ppm, MAH 1 w/w%.

Figure 13 shows the influence of the initial concentration of MAH on *ANGC*. For the whole range considered for this process variable, nearly all the population of chains remains ungrafted. Only a small fraction, around 2-4 %, exhibit one graft, and an even smaller percentage have multiple grafts (0.5-1 %). It is observed that as the concentrations of MAH increase, the number of grafts per chain also increases. The same tendencies are observed when increasing the initial PO concentration. This is probably because, for the first variable, the MAH concentration affects grafting reactions (reactions (9) and (10)) directly, and a higher PO concentration results in a larger radical population that could potentially become grafted. The variable *ANGC* presents a similar profile to the one in Figure 13 for a given reaction time, but increasing the reaction time shows no noticeable effect after 15 minutes.

This article is protected by copyright. All rights reserved.

15213919, ja, Downloaded from https://onlinelibrary.wiley.com/doi/10.1002/mats.202300018 by MARIANO ASTEASUAIN - CONICET Consejo Nacional de Investigaciones , Wiley Online Library on [02/06/2023]. See the Terms and Conditions (https://onlinelibrary.wiley.com/terms-and-conditions) on Wiley Online Library for rules of use; OA articles are governed by the applicable Creative Commons License

Accepted Article

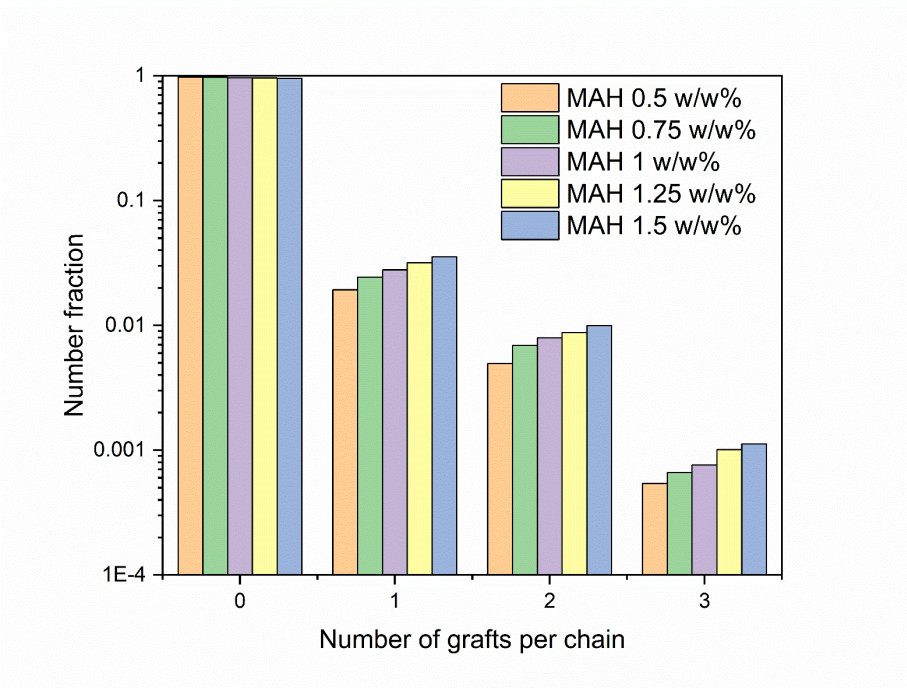


Figure 13. Effect of the initial concentration of MAH on the number of grafts per chain. PO 500 ppm, t=15 min.

6. Conclusion

A Monte Carlo model of the grafting of MAH onto PP, which considers a comprehensive set of kinetic steps, was successfully developed. The model predicts $\overline{M_n}$, $\overline{M_w}$, *DG*, *MWD*, and detailed information on the grafting distribution. A sensitivity analysis was conducted to determine the importance of the different kinetic steps, with homopolymerization, β-scission, chain grafting, and termination by disproportionation being the most significant. Chain transfer to polymer and termination by combination reactions were negligible when the reactant was the copolymer. The most significant kinetic constants were adjusted to fit experimental data, obtaining a very good representation of the experimental information. The Surface Response Method was utilized as an optimization procedure for the parameter estimation. The impact of PO and MAH initial concentrations and reaction time on polymer and graft properties was also assessed, revealing that PO concentration has significant effect on $\overline{M_n}$ and $\overline{M_w}$, and a modest influence on *DG*. On the other hand, MAH concentration has a great impact on $\overline{M_n}$, $\overline{M_w}$ and *DG*, while the reaction time has a negligible effect after 15 minutes.

Finally, it is worth highlighting the potential of the method described in this study for modeling post-reactor modification of polymers. Extending it to other systems would only require selecting the appropriate kinetic steps for the mathematical model. This procedure is straightforward.

This article is protected by copyright. All rights reserved.

15213919, ja, Downloaded from https://onlinelibrary.wiley.com/doi/10.1002/mats.202300018 by MARIANO ASTEASUAIN - CONICET Consejo Nacional de Investigaciones , Wiley Online Library on [02/06/2023]. See the Terms and Conditions (https://onlinelibrary.wiley.com/terms-and-conditions) on Wiley Online Library for rules of use; OA articles are governed by the applicable Creative Commons License

Accepted Article

Acknowledgements

This work was supported financially by Consejo Nacional de Investigaciones Científicas y Técnicas of Argentina (CONICET) (PIP 11220170100123CO), Agencia Nacional de Promoción Científica y Tecnológica of Argentina (ANPCyT) (PICT-2018-02921 and PICT-2017-0256), and Universidad Nacional del Sur (UNS) (PGI 27/M170).

7. References

[1] T. Bray, S. Damiris, A. Grace, G. Moad, M. O'Shea, E. Rizzardo, G. Van Diepen, *Macromol. Symp.* **1998**, *129*, 109.

[2] G. Moad, *Prog. Polym. Sci.* **1999**, *24*, 81.

[3] M. Van Duin, *Macromol. Symp.* **2003**, *202*, 1.

[4] B. Rainglet, Y. Chalamet, V. Bounor-Legaré, K. Delage, C. Forest, P. Cassagnau, *Polymer* **2021**, *218*, 123496.

[5] B. Rainglet, L. Verron, Y. Chalamet, V. Bounor‐Legaré, K. Delage, C. Forest, P. Cassagnau, *Macromol. React. Eng.* **2022**, *16*, 2200004.

[6] J. Guapacha, M. D. Failla, E. M. Vallés, L. M. Quinzani, *J. Appl. Polym. Sci.* **2014**, *131*, 40357.

[7] F. Berzin, J.-J. Flat, B. Vergnes, *J. Polym. Eng.* **2013**, *33*, 673.

[8] S. Bettini, J. Agnelli, *J. Appl. Polym. Sci.* **1999**, *74*, 256.

[9] A. Machado, J. Covas, M. Van Duin, *Polymer* **2001**, *42*, 3649.

[10] W. Heinen, C. H. Rosenmöller, C. B. Wenzel, H. J. M. De Groot, J. Lugtenburg, M. Van Duin, *Macromolecules* **1996**, *29*, 1151.

[11] F. Severini, M. Pegoraro, L. Yuan, G. Ricca, N. Fanti, *Polymer* **1999**, *40*, 7059.

[12] S. Bettini, J. Agnelli, *J. Appl. Polym. Sci.* **1999**, *74*, 247.

[13] S. H. P. Bettini, J. A. M. Agnelli, *J. Appl. Polym. Sci.* **2002**, *85*, 2706.

[14] K. Cao, Z.-c. Shen, Z. Yao, B.-w. Qu, X.-b. Pang, Z.-q. Lu, Y. Li, Z.-h. Chen, *Chem. Eng. Sci.* **2010**, *65*, 1621.

[15] Y. Güldoğan, S. Eğri, Z. M. Rzaev, E. Pişkin, *J. Appl. Polym. Sci.* **2004**, *92*, 3675.

This article is protected by copyright. All rights reserved.

15213919, ja, Downloaded from https://onlinelibrary.wiley.com/doi/10.1002/mats.202300018 by MARIANO ASTEASUAIN - CONICET Consejo Nacional de Investigaciones , Wiley Online Library on [02/06/2023]. See the Terms and Conditions (https://onlinelibrary.wiley.com/terms-and-conditions) on Wiley Online Library for rules of use; OA articles are governed by the applicable Creative Commons License

Accepted Article

[16] L. Krause-Sammartino, J. Lucas, M. Reboredo, M. Aranguren, *Plast. Rubber Compos.* **2006**, *35*, 117.

[17] Q.-L. Ni, J.-Q. Fan, H. Niu, J.-Y. Dong, *J. Appl. Polym. Sci.* **2011**, *121*, 2512.

[18] A. Oromiehie, H. Ebadi-Dehaghani, S. Mirbagheri, *Int. J. Chem. Eng. Appl.* **2014**, *5*, 117.

[19] R. Pruthtikul, P. Liewchirakorn, "Preparation of polypropylene graft maleic anhydride (PP-g-MA) via twin screw extrusion", in *Advanced Materials Research*, Trans Tech Publ, 2010, p. 93/451.

[20] K. E. Russell, *J. Polym. Sci., Part A: Polym. Chem.* **1995**, *33*, 555.

[21] D. Shi, R. Li, Y. Zhu, Z. Ke, J. Yin, W. Jiang, G. H. Hu, *Polym. Eng. Sci.* **2006**, *46*, 1443.

[22] S. N. Sathe, G. S. S. Rao, S. Devi, *J. Appl. Polym. Sci.* **1994**, *53*, 239.

[23] M. Zhang, R. H. Colby, S. T. Milner, T. C. M. Chung, T. Huang, W. Degroot, *Macromolecules* **2013**, *46*, 4313.

[24] F. L. Figueira, Y.-Y. Wu, Y.-N. Zhou, Z.-H. Luo, P. H. Van Steenberge, D. R. D'hooge, *React. Chem. Eng.* **2021**, *6*, 640.

[25] J. C. Hernández-Ortiz, P. H. M. Van Steenberge, M.-F. Reyniers, G. B. Marin, D. R. D'Hooge, J. N. E. Duchateau, K. Remerie, C. Toloza, A. L. Vaz, F. Schreurs, *AIChE J.* **2017**, *63*, 4944.

[26] S. Lee, H. Lee, T. Chang, A. Hirao, *Macromolecules* **2017**, *50*, 2768.

[27] C.-Z. Xu, J.-J. Wang, X.-P. Gu, L.-F. Feng, *AIChE J.* **2019**, *65*, e16632.

[28] J. Cha, J. L. White, *Polym. Eng. Sci.* **2001**, *41*, 1227.

[29] D. Shi, J. Yang, Z. Yao, Y. Wang, H. Huang, W. Jing, J. Yin, G. Costa, *Polymer* **2001**, *42*, 5549.

[30] R. Giudici, *Macromol. Symp.* **2007**, *259*, 354.

[31] L. G. Aguiar, P. A. Pessôa-Filho, R. Giudici, *Macromol. Theory Simul.* **2011**, *20*, 837.

[32] Y. Zhu, L. An, W. Jiang, *Macromolecules* **2003**, *36*, 3714.

[33] B. De Roover, M. Sclavons, V. Carlier, J. Devaux, R. Legras, A. Momtaz, *J. Polym. Sci., Part A: Polym. Chem.* **1995**, *33*, 829.

[34] B. D. Roover, J. Devaux, R. Legras, *J. Polym. Sci., Part A: Polym. Chem.* **1996**, *34*, 1195.

This article is protected by copyright. All rights reserved.

15213919, ja, Downloaded from https://onlinelibrary.wiley.com/doi/10.1002/mats.202300018 by MARIANO ASTEASUAIN - CONICET Consejo Nacional de Investigaciones , Wiley Online Library on [02/06/2023]. See the Terms and Conditions (https://onlinelibrary.wiley.com/terms-and-conditions) on Wiley Online Library for rules of use; OA articles are governed by the applicable Creative Commons License

Accepted Article

[35] Y. Minoura, M. Ueda, S. Mizunuma, M. Oba, *J. Appl. Polym. Sci.* **1969**, *13*, 1625.

[36] R. Ho, A. Su, C. Wu, S. Chen, *Polymer* **1993**, *34*, 3264.

[37] R. Zhang, Y. Zhu, J. Zhang, W. Jiang, J. Yin, *J. Polym. Sci., Part A: Polym. Chem.* **2005**, *43*, 5529.

[38] J. C. Hernández-Ortiz, P. H. M. Van Steenberge, J. N. E. Duchateau, C. Toloza, F. Schreurs, M.-F. Reyniers, G. B. Marin, D. R. D'Hooge, *Chem. Eng. J.* **2019**, *377*.

[39] F. L. Figueira, A. D. Trigilio, Y.-Y. Wu, Y.-N. Zhou, Z.-H. Luo, P. H. M. Van Steenberge, D. R. D'Hooge, *Chem. Eng. J.* **2023**, *452*, 139389.

[40] M. S. Kellou, G. Jenner, *Eur. Polym. J.* **1976**, *12*, 883.

[41] C. W. Lin, W. L. Lee, *J. Appl. Polym. Sci.* **1998**, *70*, 383.

[42] A. Machado, M. Van Duin, J. Covas, *J. Polym. Sci., Part A: Polym. Chem.* **2000**, *38*, 3919.

[43] A. V. Machado, J. A. Covas, M. Van Duin, *J. Appl. Polym. Sci.* **2001**, *81*, 58.

[44] Y.-Y. Wu, F. L. Figueira, M. Edeleva, P. H. M. Van Steenberge, D. R. D'hooge, Y.-N. Zhou, Z.-H. Luo, *AIChE J.* **2022**, *68*, e17559.

[45] C.-X. Zhu, Y.-Y. Wu, F. L. Figueira, P. H. M. Van Steenberge, D. R. D'Hooge, Y.-N. Zhou, Z.-H. Luo, *Chem. Eng. J.* **2022**, *444*, 136595.

[46] J. Wang, Y. Ren, Y. Yang, X. Fan, B. Jiang, Z. Huang, J. Wang, Y. Yang, *AIChE J.* **2023**, e18111.

[47] D. Meimaroglou, C. Kiparissides, *Macromolecules* **2010**, *43*, 5820.

[48] H. Tang, W. Dai, B. Chen, *Polym. Eng. Sci.* **2008**, *48*, 1339.

[49] L. C. Simon, J. B. P. Soares, *Ind. Eng. Chem. Res.* **2005**, *44*, 2461.

[50] J. Keum, J. L. White, *J. Vinyl Addit. Technol.* **2005**, *11*, 143.

[51] A. Aboulkas, A. El Bouadili, *Energy Convers. Manage.* **2010**, *51*, 1363.

[52] D. T. Gillespie, *J. Phys. Chem. A* **1977**, *81*, 2340.

[53] M. J. Krell, A. Brandolin, E. M. Valles, *Polym. React. Eng.* **1994**, *2*, 389.

[54] T. Romero Pietrafesa, A. Brandolin, C. Sarmoria, M. Asteasuain, "Polypropylene Grafted with Maleic Anhydride: A Stochastic Model", in *2022 AIChE Annual Meeting*, Phoenix, EE. UU., 2022.

This article is protected by copyright. All rights reserved.

15213919, ja, Downloaded from https://onlinelibrary.wiley.com/doi/10.1002/mats.202300018 by MARIANO ASTEASUAIN - CONICET Consejo Nacional de Investigaciones , Wiley Online Library on [02/06/2023]. See the Terms and Conditions (https://onlinelibrary.wiley.com/terms-and-conditions) on Wiley Online Library for rules of use; OA articles are governed by the applicable Creative Commons License

Accepted Article

[55] Y.-Y. Wu, F. L. Figueira, P. H. M. Van Steenberge, D. R. D'Hooge, Y.-N. Zhou, Z.-H. Luo, *Chem. Eng. J.* **2021**, *425*, 130463.

[56] S. Wu, K. A. McLean, T. J. Harris, K. B. McAuley, *Int. J. Adv. Mechatron. Syst.* **2011**, *3*, 188.

[57] K. Z. Yao, B. M. Shaw, B. Kou, K. B. McAuley, D. Bacon, *Polym. React. Eng.* **2003**, *11*, 563.

[58] G. Franceschini, S. Macchietto, *Chem. Eng. Sci.* **2008**, *63*, 4846.

[59] J. L. Hart, A. Alexanderian, P. A. Gremaud, *SIAM J. Sci. Comput.* **2017**, *39*, A1514.

[60] V. Todorov, I. Dimov, T. Ostromsky, S. Apostolov, R. Georgieva, Y. Dimitrov, Z. Zlatev, *Neural. Comput. Appl.* **2021**, *33*, 1999.

[61] M. Redhe, M. Giger, L. Nilsson, *Struct. Multidiscipl. Optim.* **2004**, *27*.

[62] K. Marti, "*Stochastic optimization methods*", Springer Berlin, Heidelberg, 2008.

[63] G. E. Box, J. S. Hunter, W. G. Hunter, "Statistics for experimenters", in *Wiley Series in Probability and Statistics*, Wiley Hoboken, NJ, 2005.

[64] M. H. Kutner, C. J. Nachtsheim, J. Neter, W. Wasserman, "*Applied linear regression models*", McGraw-Hill/Irwin New York, 2004.

[65] R. Unal, R. Lepsch, M. McMillin, "Response surface model building and multidisciplinary optimization using D-optimal designs", in *7th AIAA/USAF/NASA/ISSMO Symposium on Multidisciplinary Analysis and Optimization*, 19984759.

This article is protected by copyright. All rights reserved.

15213919, ja, Downloaded from https://onlinelibrary.wiley.com/doi/10.1002/mats.202300018 by MARIANO ASTEASUAIN - CONICET Consejo Nacional de Investigaciones , Wiley Online Library on [02/06/2023]. See the Terms and Conditions (https://onlinelibrary.wiley.com/terms-and-conditions) on Wiley Online Library for rules of use; OA articles are governed by the applicable Creative Commons License